The Mechanisms of miR-638/StarD10 in HDL Metabolism

Ping Ye (yeping301@sina.com)
Department of Geriatric Cardiology, National Clinical Research Center for Geriatric Diseases Chinese PLA General Hospital, Beijing, China National Clinical Research Center for Geriatric Diseases
https://orcid.org/0000-0003-4974-7087

Xiaona Wang
Chinese PLA General Hospital

Jie Han
the second affiliated hospital of xian jiaotong university

Ruihua Cao
Chinese PLA General Hospital

Yongyi Bai
Chinese PLA General Hospital

Research

Keywords: MiR-638, StarD-10, HDL metabolism

Posted Date: January 18th, 2021

DOI: https://doi.org/10.21203/rs.3.rs-142814/v1

Abstract

Background: MicroRNA (miRNA) plays an important role in regulation of genes, especially in post-transcriptional level. Many studies had studied the role of miRNAs in the development and progression of cardiovascular disease through miRNA knockout mice models, and chemically synthesized mimics or inhibitors of miRNAs. This study was designed to further investigate the effect of miR-638 on lipid metabolism-related gene expression.

Methods: miR-638 mimics and inhibitors were transfected into HepG2 and macrophages. Appropriate concentrations and time points used to treat cells were determined through pre-experiment. Then RT2 Profiler™ PCR Array chips contained 84 human lipoprotein signals and cholesterol metabolism related gene were used to investigate the effect of miR-638 on lipid metabolism. Real-time PCR and Western blot were also used to verify the results.

Mice received 2 times tail vein injections of StarD10 mimics and inhibitors the first week, and the injection continued three weeks with one time foreach week. Total plasma cholesterol, triglyceride, LDL-C and HDL-C levels were obtained at sacrifice; All mice were injected intraperitoneally with H3-cholesterol–labeled and cholesterol -loaded raw 264.7 macrophages (0.5m L /mice). Serum, liver tissues and feces were collected at 24 hour. All samples were analyzed for the appearance of 3H-tracer (as the percentage of the total injected counts). Protein were extracted from liver tissue, and Western-blot was conducted to evaluate lipid metabolism related protein expression. Sacrificed the mice and removed the aortas, aorta plaque and macrophage were investigated by examination of stained sections by H-E staining, Oil-red O staining and CD68+ staining.

Results: Transfected miR-638 Mimics in HepG2 cells and macrophages could significantly increase the expression of miR-638. Transfected miR-638 Inhibitors in HepG2 cells could significantly decreased the expression of miR-638. Results showed that transfected miR-638 Mimics in HepG2 cells and macrophages could reduce the RNA and protein expression levels of ATP-binding cassette A-1 (ABCA1), ATP-binding cassette G-1 (ABCG1) and very low density lipoprotein receptor (VLDLR), and transfected miR-638 Inhibitors in HepG2 cells could increase the RNA and protein expression levels of ABCA1 and ABCG1.

Compared with the control groups, the levels of LDL-C and TC were decreased lightly, while the level of HDL3-C/HDL-C was increased in the StarD10 mimics group. The amount of 3H-cholesteral in StarD10 mimics group were increased by 62.86% in the plasma, 30.73% in the liver and 52.72% in the feces, respectively. The expression of ABCA1, ABCG1, protein in the liver was higher in StarD10 mimics. The ratio of the plaque area to luminal area of mice in the StarD10 mimics group is slighter smaller than that of the adenovirus control group, but there is no statistical difference ($P > 0.05$). Compared with mice in the adenovirus control group, mice in the StarD10 mimics group have much lower lipid content ($P < 0.01$) and macrophage content ($P < 0.01$) in the plaque.

Conclusions: MiR-638/StarD10 could influence the expression levels of genes related to lipid metabolism. MiR-638/StarD10 can influence the blood lipid level, promote reverse transport of cholesterol, and StarD10 can reduce macrophage content and lipid content in the active surface patches in the mice.

Introduction

A large number of clinical and epidemiological studies have confirmed [1,2] that an increase in plasma low-density lipoprotein cholesterol (LDL-C) levels can accelerate the occurrence of atherosclerosis (AS), and a decrease in plasma high-density lipoprotein cholesterol (HDL-C) levels can lead to an increase in the incidence of AS. HDL exerts its anti-atherosclerotic role by participating in reverse cholesterol transport (RCT). In addition to its anti-atherosclerotic effect, HDL also has an organ-protective effect. Our recent research shows the following that low HDL-C increased the incidence of subclinical myocardial injury, lower left ventricular diastolic function and cerebral hemorrhage [3-5]. Although a large number of epidemiological studies have confirmed that abnormal HDL metabolism is an important cardiovascular risk factor, the mechanism governing HDL metabolic disorders has not been fully elucidated. Therefore, it is urgently important to conduct in-depth translational research on HDL metabolism and to clarify the pathogenesis of low HDL to guide the development of effective prevention and treatment methods and to promote human health.

Recent studies have found that microRNAs (miRNAs) are closely related to the regulation of human HDL metabolism. miRNAs may be a potential target for the treatment of HDL metabolic disorders. Some studies have reported that certain miRNAs are related to cholesterol metabolism, such as miR-33, miR-370, miR-122, miR-335, and miR-143. At the cell and organismal level, more research has been performed on miR-33. miR-33 regulates the HDL metabolic pathway by inhibiting the expression of the ABCA1 gene [6]. Inhibiting miR-33 can increase the plasma HDL-C level by increasing the ABCA1 cholesterol reverse transport pathway. However, the metabolic regulation of HDL is achieved not by a single gene encoding miR-33 but by multiple genes.

Moreover, the miRNA screening in the above studies all started with the differential expression of miRNA in cell models. However, in the real world, patients with clinical dyslipidemia are in a complex interaction between internal and external factors, and miRNAs are not continuously and stably expressed. It shows a certain chronology with disease or internal and external environment changes. Therefore, screening only from cell models may lose some important information and omit miRNAs that are closely related to clinical HDL metabolic abnormalities. Recently, with the deepening of serum/plasma miRNA research [7,8], the research strategy of circulating miRNAs based on patients has become a reality. Based on the circulating miRNA research strategy, we have performed miRNA screening related to HDL metabolism and found that the difference in the expression of miR-638 between subjects with low HDL-C and subjects with normal HDL-C was significant. We also found that the target of mir-638 in regulating HDL metabolism is due to steroid hormone synthesis of acute regulatory protein associated steroidogenic acute regulatory protein-related lipid transfer domain 10 (StarD10) by Bioinformatics (http://www.

targetscan.org/). Therefore, we focused on miR-638/StarD10 in this study and explored its relationship with HDL metabolism through in vitro and in vivo experiments.

Results

Effects of miR-638 on the expression of genes related to lipid metabolism in HepG2 cells and macrophages

To further explore the role of miR-638 in lipid metabolism, in this study, miR-638 mimics and inhibitors were transfected into HepG2 cells and macrophages. Changing the concentration and treatment time can effectively increase or decrease the content of miR-638 in cells (Figure 1). An RT² Profiler PCR Array chip containing 84 key genes involved in lipoprotein transport and cholesterol metabolism was subsequently employed to detect genes related to lipid metabolism in cells transfected with miR-638 mimics and inhibitors. The level of expression was changed, and real-time PCR and Western blot analyses were employed to further verify the chip results at the RNA and protein levels. The results showed the following: 1) miR-638 mimics/inhibitors can significantly increase/decrease the expression level of miR-638 in HepG2 cells after transfection in HepG2 cells. After further repeated verification, it was found that transfection of miR-638 mimics can reduce ABCA1 and ABCG1 RNA and protein expression levels, while transfection of miR-638 inhibitors can increase the expression levels of ABCA1 and ABCG1 RNA and protein (Figure 2). 2) Transfection of miR-638 mimics into macrophages can significantly increase macrophage miR-638 expression levels. After further verification, it was found that transfection of miR-638 mimics can reduce the expression levels of ABCA1 and ABCG1 RNA and protein (Figure 3).

Effect of miR-638 on cholesterol efflux in *HepG2 cells and macrophages*

Fluorescence labeled cholesterol (NBD-cholesterol) was used to evaluate the effect of mir-638 on the cholesterol efflux. HepG2 cells and macrophages were treated with miR-638 mimics and inhibitors and miR-638 mimics/inhibitor negative controls, and cells were loaded with ox-LDL at 100 μg/mL and incubated with NBD-cholesterol. Cholesterol efflux was induced by ApoAI-induced efflux fluid, HDL-induced efflux fluid, and standard serum-induced efflux fluid. In HepG2 cells, miR-638 mimics was observed to inhibit ABCA1-mediated cholesterol outflow to ApoAI and ABCG1-mediated cholesterol outflow to HDL, while miR-638 inhibitors was determined to promote ABCA1-mediated cholesterol outflow to ApoAI and ABCG1-mediated cholesterol outflow to HDL (Figure 4). Also, miR-638 mimics was able to inhibit ABCA1-mediated cholesterol efflux to ApoAI in macrophages (Figure 5).

Study on the relationship between miR-638 and STARD10

The Luc/R-Luc expression in 3'UTR STARD10-WT +miR-638 mimics group and 3'UTR STARD10-MUT + miR-638 mimics group was lower than normal control group (respectively $P<0.001$ and $P=0.03$). The Luc/R-Luc expression in 3'UTR STARD10-WT +miR-638 mimics group was lower than 3'UTR STARD10-MUT + miR-638 mimics group ($P=0.013$) (Figure 6). After 24 hours intervened in human HepG2 cells,

compared with the control group, the expression of STARD10 protein decreased in miR-638 mimic group (P=0.004), and increased in miR-638 inhibitor group (P=0.008) (Figure 6).

Effect of StarD10 on blood lipids in mice

We further studied in vivo. Since there is no mir-638 in mice, StarD10, its downstream target, was selected as the research object. Four weeks after the tail vein injection of the adenovirus-packaged StarD10 vector, the blood lipid levels of the mice changed significantly. Compared with the baseline group, the PBS control group, and the adenovirus control group, the plasma TC and LDL-C in the StarD10 inhibitor group decreased slightly (Table 1), and the HDL3-C/HDL-C ratio increased (Table 2).

Effects of StarD10 on cholesterol reverse transport in mice

By measuring the percentage of ^{3}H-cholesterol in the serum, liver and feces of mice as a percentage of total ^{3}H-cholesterol injected intraperitoneally, reverse cholesterol transport was evaluated in vivo. After the mice were successfully modeled, the plasma ^{3}H-cholesterol distribution of mice in each group at 6 h, 24 h, and 48 h after intraperitoneal injection of isotope-labeled RAW264.7 cells was determined, as shown in Table 3. Six and 24 h after injection of isotope-labeled cells, the serum ^{3}H-cholesterol content of mice in each group increased slightly; 48 h after injection of isotope-labeled cells, the serum ^{3}H-cholesterol content in the mice of each group increased significantly. Compared with the adenovirus control group, the serum ^{3}H-cholesterol content of the StarD10 inhibitor group exhibited no significant differences at 6 h and 24 h; compared with the adenovirus control group, the serum ^{3}H-cholesterol content of the StarD10 inhibitor group increased by 62.86% ($P < 0.01$) at 48 h, and there were no significant differences among the StarD10 mimic group, the PBS control group and the adenovirus control group (Figure 7).

The amount of ^{3}H-cholesterol remaining in the liver 48 h after the injection of ^{3}H-cholesterol-labeled macrophages into mice, as well as the content of ^{3}H-cholesterol in the feces collected within 48 h (as a percentage of the total ^{3}H-cholesterol injected), were determined experimentally (Table 4). Compared with the adenovirus control group, the residual ^{3}H-cholesterol content in the liver of the StarD10 inhibitor group increased by 30.73% ($P < 0.01$). There was no significant difference between the StarD10 mimic group and the adenovirus control group (Figure 7); ^{3}H-cholesterol excretion increased by 52.72% in two days ($P < 0.01$). Also, there was no significant difference between the mice in the StarD10 mimics group and the adenovirus control group, as shown in Figure 7.

Effect of StarD10 on liver metabolism-related proteins in mice

ABCA1 protein expression in liver tissues of the PBS control group, the adenovirus control group, the StarD10 inhibitor group and the StarD10 mimic group were 0.724 ± 0.016, 1.079 ± 0.037, 1.501 ± 0.030, and 1.047 ± 0.030, respectively. The expression of ABCA1 protein in the StarD10 inhibitor group was significantly higher than that in the other groups, ($P < 0.01$) (Figure 8). There were no significant

differences in ABCA1 protein expression among the PBS control group, the adenovirus control group and the StarD10 mimic group.

The levels of ABCG1 protein expression in the PBS control group, the adenovirus control group, the StarD10 inhibitor group and the StarD10 mimic group in liver tissue were 0.319 ± 0.012, 0.466 ± 0.021, 1.157 ± 0.03, and 0.671 ± 0.03, respectively. The expression of ABCG1 protein in the StarD10 inhibitor group was significantly higher than that in the other groups ($P < 0.01$) (Figure 8). There were no significant differences in ABCA1 protein expression among the PBS control group, the adenovirus control group and the StarD10 mimic group.

Effect of StarD10 on aortic plaque in mice

The ratio of the plaque area to the lumen area in the StarD10 inhibitor group was slightly lower than that in the adenovirus control group, and no significant difference was observed ($P > 0.05$) (Figure 8). The StarD10 inhibitor group had a significantly lower lipid content in plaques than did the adenovirus control group ($P < 0.01$), and the macrophage content in plaques was significantly lower than that in the virus control group ($P < 0.01$) (Figure 9). The lipid content in the plaques of the StarD10-silenced mice was not significantly different from that of the adenovirus control group, and the macrophage content in the plaque was slightly higher than that of the adenovirus control group ($P = 0.035$) (Figure 9).

Discussion

miRNA is a type of evolutionarily conserved non-coding small RNA, which is transcribed from intergenic regions, introns, and exon regions encoding proteins, and has the function of regulating gene expression at the translation level[9]. Recent studies have found that miRNAs are closely related to a variety of cardiovascular diseases in humans [10]. With the gradual understanding of miRNA, its regulatory effect on HDL metabolism has also been gradually confirmed. miRNA may become a potential therapeutic target for regulating HDL metabolic disorders and other diseases. This topic mainly starts with the differential expression of human plasma miRNA, and screens circulating miR-638 related to HDL metabolism in hemorrhagic plasma through miRNA chip technology. Through bioinformatics target prediction and cell experiments, it is confirmed that the steroid hormone synthesis acute regulatory protein-related lipid transport domain protein 10 (STARD10) is the target gene of miR-638. It provides a research basis for further exploring the effect of miR-638 on the expression of lipid metabolism related genes.

In cell experiment, we found that miR-638 could affect the expression of lipid metabolism related genes in HepG2 cells and macrophages. Transfection of miR-638 mimic in HepG2 cells and macrophages significantly increased the expression level of miR-638 in HepG2 cells and macrophages, and significantly decreased the expression level of miR-638 in HepG2 cells after transfection with miR-638 inhibitor. Results showed that transfected miR-638 Mimics in HepG2 cells and macrophages could reduce the RNA and protein expression levels of ATP-binding cassette A-1 (ABCA1), ATP-binding cassette G-1 (ABCG1), and transfected miR-638 Inhibitors in HepG2 cells could increase the RNA and protein

expression levels of ABCA1 and ABCG1. In animal experiments, adenovirus packaging StarD10 Mimics/inhibitor can be transfected into $LDLr^{-/-}$ mouse liver; StarD10 Mimics is a favorable factor for mouse lipid metabolism, which can promote reverse cholesterol transport through ABCA1, ABCG1, increase the ratio of HDL3-C/HDL, and can improve the lipid content in mouse aortic plaque and reduce inflammation in the plaque.

Previous studies on miRNA and lipid metabolism (especially HDL metabolism) have been published[11,12]. miR-33 is the most deeply studied miRNA related to HDL metabolism[13]. The intracellular miR-33 genes include miR-33a and miR-33b. miR-33 regulates HDL metabolism by inhibiting the expression of ABCA1 gene[14-16]. Overexpression of miR-33a in cells can inhibit the expression of ABCA1 gene and protein, whereas inhibition of intracellular miR-33a level can promote the expression of ABCA1 gene and protein. miR-33b is only present in human SREBP-1 genes and plays a more important role in triglyceride synthesis and metabolism[17,18]. Animal experiments showed that after miR-33 was inhibited, the expression of ABCA1 gene and protein in liver was up-regulated, and the plasma HDL-C level was increased by 40%. In addition, inhibition of miR-33 expression in mice can also increase the expression of ABCA1 in macrophages of atherosclerotic plaque and accelerate the clearance of cholesterol in plaque macrophages, thus promoting the regression of atherosclerotic plaque. Inhibiting the expression of miR-33a and miR-33b in African green monkey can also up regulate the expression of ABCA1 gene and protein in liver, thus further promoting the plasma HDL-C level of African green monkey[19]. In addition, mir-370, MiR-27, miR-335, miR-143, mir-122[20-29] were also found to be related to lipid metabolism. The miRNA screening in the above research starts from the differential expression of miRNA in cell model. However, in the real world, patients with clinical dyslipidemia are in complex internal and external interaction, and miRNA is not expressed stably, but is in a certain time sequence with the changes of disease or internal and external environment. Therefore, screening from cell model may lose some important information and miss miRNA closely related to clinical HDL metabolic abnormality. In recent years, with the further research of serum/plasma miRNA [7,8], the research strategy of circulating miRNAs based on patients has become a reality. Based on the circulating miRNA research strategy, we have performed miRNA screening related to HDL metabolism and found that the difference in the expression of miR-638 between subjects with low HDL-C and subjects with normal HDL-C was significant. At present, most of the studies on mir638 are focused on breast cancer[30], but few studies on mir638 and lipid metabolism[31]. miR638 We also found that the target of mir-638 in regulating HDL metabolism is due to steroid hormone synthesis of acute regulatory protein associated steroidogenic acute regulatory protein-related lipid transfer domain 10 (StarD10) by Bioinformatics (http://www. targetscan.org/). Therefore, we focused on miR-638/StarD10 in this study and explored its relationship with HDL metabolism through in vitro and in vivo experiments.

Adenosine triphosphate binding cassette transporter A1(ABCA1) located in the basement membrane of cells can transport intracellular cholesterol to extracellular apoA □ and form pre-β-HDL, this is the first step in synthesizing HDL. ABCA1 is a transmembrane transporter, which is composed of two interconnected functional units. Each functional unit contains a transmembrane domain and an intracellular adenosine

triphosphate (ATP) binding domain, which provides energy for transmembrane transport by binding with intracellular ATP[32-35]. As an important molecule involved in HDL synthesis, ABCA1 mutation at gene level can lead to a familial high-density lipoprotein deficiency syndrome called Tangier disease, which is characterized by complete loss of HDL in plasma and severe lipid metabolism disorder[33-35]. In addition to ABCA1, ATP binding cassette transporter G1 (ABCG1) also plays an important role in HDL metabolism. In vitro, ABCG1 and ABCA1 could synergistically mediate cholesterol efflux to HDL. The lack of both ABCA1 and ABCG1 in mice will cause a large number of macrophage-derived foam cells to accumulate in the spleen, heart, lymph nodes, liver and lungs[36-39]. This study confirmed that ABCA1 and ABCG1 play an important role in HDL metabolism at the level of cell and animal experiments.

The initial hypothesis that increasing total HDL-C levels might reduce cardiovascular events in patients with coronary heart disease was largely based on primary prevention observational studies in which increasing HDL-C levels reduced coronary heart disease risk. However, recent studies have shown that elevated HDL-C alone does not reduce the risk of adverse events in patients with coronary heart disease. Such studies as ILLUMINATE[40], dal-OUTCOMES[41], and HPS2-THRIVE [42], which evaluated elevated HDL-C for the treatment of acute coronary syndromes or atherosclerotic diseases, have found that despite significant increases in HDL-C, HDL-C failed to achieve clinical benefits. Previous studies have divided HDL into different subclasses based on differences in shape, size, density, and function[43]. HDL2 and HDL3 are the main subclasses of HDL in normal human plasma. The clinical functions and metabolism of different subclasses are different. Compared with HDL2-C, HDL3-C has a higher density and smaller particles, accounting for 78% of the total HDL-C. HDL2 and HDL3 have different anti-atherosclerotic mechanisms. Changes in the HDL2/HDL3 ratio can cause changes in the risk of atherosclerotic diseases, but this possibility is controversial. Some studies suggest that HDL2 mediates cholesterol outflow through the ABCA1, ABCG1, and SR-BI pathways[44-46] and thus plays an important role in reverse cholesterol transport. These views suggest that HDL2 is more anti-atherosclerotic than HDL3. In contrast, HDL3 has higher anti-inflammatory and antioxidant effects than HDL2[47,48]. A recent article published in the European Journal of Cardiology suggested that HDL3 has higher levels of antioxidant proteins (such as serum paraoxonase/aryl esterases 1 and 3) and can inhibit low-density lipoprotein oxidation compared to HDL2. An increased risk of myocardial infarction or death is associated with low levels of HDL3-C but not with low levels of HDL2-C[49]. The comprehensive lipid and RCT results indicate that StarD10 can play an anti-atherosclerotic role by increasing the HDL3-C/HDL-C ratio and promoting the cholesterol reverse transport pathway.

As a class of small noncoding single-stranded RNAs, miRNAs can play an important role in regulating gene expression. Not only can miRNAs be regulated at the posttranscriptional level, but they can also change the transduction of cell signals[50-60]. Therefore, miRNAs can be potential therapeutic targets, and more miRNAs involved in regulating lipid metabolism-related pathways will be identified in future research. Although research on these miRNAs faces many challenges, they have good development prospects. Identifying miRNAs and their corresponding target genes related to lipid metabolism, regulating the expression of these miRNAs, and modifying their structures may facilitate the treatment of lipid metabolism disorders. This project may also continue to explore the results of lipid metabolism-

related gene chips transfected with miR-638/StarD10 mimics and inhibitors and further study the effect of miR-638/StarD10 on lipid metabolism.

Experimental Method

Cell experiment part:

In HepG2 cells: According to the pre-experiment results, the concentration of miR-638 Mimics was selected as M3 (20nM), and the concentration of miR-638 Inhibitors was selected as I3 (100nM). MiR-638 Mimics/ Inhibitors Negative Control transfection was performed using the same treatment concentration and time. After transfection, RNA was extracted from HepG2 cells and detected by Real-time PCR chip. The human lipoprotein signal and cholesterol metabolism RT² Profiler ™ PCR Array chip contains 84 key genes involved in lipoprotein transport and cholesterol metabolism. Detection of RNA concentration and purity of each group: According to the ratio of OD260 / OD280, determine whether the purity of the extracted RNA meets the requirements. The OD260 / OD280 of good-purity RNA should be between 1.7-2.0. 1% RNA agarose gel electrophoresis can be used to check the integrity of the extracted RNA and whether it is contaminated by protein or DNA. Further verification: According to the pre-experiment results, the concentration of miR-638 Mimics was selected as M3 (20nM), the concentration of miR-638 Inhibitors was selected as I3 (100nM), and the processing time was selected for 48 hours. MiR-638 Mimics/Inhibitors Negative Control transfection was performed using the same treatment concentration and time. After transfection, RNA was extracted from HepG2 cells, and real-time PCR (Real-time PCR) was performed. After transfection, HepG2 cell proteins were extracted for Western blot.

Effect of miR-638 on cholesterol efflux in HepG2 cells: According to the pre-experiment results, the concentration of miR-638 Mimics was selected as M3 (20nM), the concentration of miR-638 Inhibitors was selected as I3 (100nM), and the treatment time was selected for 48 hours. MiR-638 Mimics / Inhibitors Negative Control transfection was performed using the same treatment concentration and time. Discard the old culture medium, add autoclaved 1 × PBS to wash the cells 2-3 times and aspirate. HepG2 cells were starved for 8 hours in serum-free medium. Discard the old culture solution, add autoclaved 1 × PBS to wash the cells 2-3 times and aspirate. Replace the DMEM + 10% FBS complete culture solution with a concentration of 100μg / mL ox-LDL, and place it in a carbon dioxide cell incubator at 37ºC, 5% CO_2, and 95% relative humidity for 24 hours. Add 100 μM scavenger receptor SR-BI inhibitor BLT-1 to the cells using HDL-induced effluent and incubate the cells for 2 hours. Add autoclaved 1 × PBS to wash the cells 2-3 times and aspirate. A 5 μM NBD-cholesterol incubation solution was prepared with DMEM culture solution, and HepG2 cells were incubated at 37 ºC for 4 hours. The incubation solution was discarded, and the cells were washed with autoclaved 1 × PBS for 2-3 times and sucked. HepG2 cells were incubated with ApoAI (25 μg / mL), HDL (50 μg / mL), and standard serum-induced effluent at 37 ºC for 4 hours. After incubation, the induced effluent was collected, centrifuged (4 ºC, 12000g, 15 minutes), cell debris was removed, and an equal amount of effluent was added to a black 96-well microtiter plate. Cells were washed 3 times in autoclaved 1 × PBS and aspirated. Lyse cells with 0.1% Triton X-100 for 30 minutes and mix by pipetting. Collect the cell lysate into a sterile centrifuge tube, centrifuge (4 ºC, 12000g,

10 minutes), collect the supernatant and add it to the black 96-well enzyme. The fluorescence intensity of induced effluent and cell lysate was measured using a fluorescence microplate reader. The excitation and emission wavelengths were 469 nm and 537 nm, respectively. Cell NBD-cholesterol efflux calculation formula: Cholesterol efflux rate = $FI_{\text{-induced efflux}}$ / ($FI_{\text{-induced effluent}}$ + $FI_{\text{cell lysate}}$) × 100%

Macrophages: According to the pre-experiment results, the concentration of miR-638 Mimics was selected as M3 (20nM), and the processing time was selected for 48 hours. The same treatment concentration and time were used for miR-638 Mimics Negative Control transfection. RNA from transfection macrophages was extracted and examined by Real-time PCR chip. Human lipoprotein signal and cholesterol metabolism RT² Profiler PCR Array chip contains 84 key genes involved in lipoprotein transport and cholesterol metabolism. Determine whether the purity of the extracted RNA meets the requirements according to the ratio of OD260 / OD280. The OD260 / OD280 of good-purity RNA should be between 1.7-2.0. 1% RNA agarose gel electrophoresis can be used to check the integrity of the extracted RNA and whether it is contaminated by protein or DNA. Further verification: According to the pre-experiment results, the concentration of miR-638 Mimics was selected as M3 (20nM), and the processing time was selected as 48 hours. The same treatment concentration and time were used for miR-638 Mimics Negative Control transfection. After transfection, RNA was extracted from macrophages cells, and real-time PCR (Real-time PCR) was performed. After transfection, macrophages cell proteins were extracted for Western blot.

Effect of miR-638 on cholesterol efflux in macrophages: According to the pre-experiment results, the concentration of miR-638 Mimics was selected as M3 (20nM), and the treatment time was selected for 48 hours. The same treatment concentration and time were used for miR-638 Mimics Negative Control transfection. Macrophage NBD-cholesterol efflux assay: Discard the old culture solution, add autoclaved 1 × PBS to wash the cells 2-3 times and aspirate. Macrophages were starved for 8 hours in serum-free medium. Discard the old culture solution, add autoclaved 1 × PBS to wash the cells 2-3 times and aspirate. Replace the DMEM + 10% FBS complete culture solution with a concentration of 100μg / mL ox-LDL, and place it in a carbon dioxide cell incubator at 37 ºC, 5% CO_2, and 95% relative humidity for 24 hours. Add 100 μM scavenger receptor SR-BI inhibitor BLT-1 to the cells using HDL-induced effluent and incubate the cells for 2 hours. Add autoclaved 1 × PBS to wash the cells 2-3 times and aspirate. The NBD-cholesterol incubation solution with a concentration of 5 μM was prepared in DMEM culture medium. After incubating HepG2 cells at 37 ºC for 4 hours, the incubation solution was discarded, and the cells were washed with autoclaved 1 × PBS for 2-3 times and sucked. Cells were incubated with ApoAI (25 μg / mL), HDL (50 μg / mL), and standard serum-induced effluent at 37 ºC for 4 hours. After incubation, the induced effluent was collected, centrifuged (4 ºC, 12000g, 15 minutes), cell debris was removed, and an equal amount of effluent was added to a black 96-well microtiter plate. Cells were washed 3 times in autoclaved 1 × PBS and aspirated. Lyse cells with 0.1% Triton X-100 for 30 minutes and mix by pipetting. Collect the cell lysate into a sterile centrifuge tube, centrifuge (4 ºC, 12000g, 10 minutes), collect the supernatant and add it to the black 96-well enzyme. The fluorescence intensity of induced effluent and cell lysate was measured using a fluorescence microplate reader. The excitation and emission

wavelengths were 469 nm and 537 nm, respectively. Cell NBD-cholesterol efflux calculation formula: Cholesterol efflux rate = $FI_{\text{-induced efflux}}$ / ($FI_{\text{-induced effluent}}$ + $FI_{\text{cell lysate}}$) × 100%

The 3UTR(STARD10) sequence was amplified using human cDNA as a template and was inserted downstream of the luciferase reporter gene in the pMIR-REPORT luciferase vector. If the addition of miR-638 to the 3UTR(STARD10) sequence affects luciferase expression, the binding site of miR-638 can be confirmed by detecting luciferase expression. A plasmid vector was constructed to detect 3UTR(STARD10) activity. The 3UTR(STARD10mut) sequence was amplified using H2183 as a template and was inserted downstream of the luciferase reporter gene in the pMIR-REPORT luciferase vector. If the addition of miR-638 to the 3UTR(STARD10mut) sequence affects luciferase expression, the binding site of miR-638 can be confirmed by detecting luciferase expression. Plasmid vectors were constructed to detect 3UTR(STARD10mut) activity. They were divided into four groups: wild-type 3'UTR of STARD10 + control; wild-type 3'UTR of STARD10 + miR-638 mimics; mutant 3'UTR of STARD10 + control; mutant 3'UTR of STARD10 + miR-638 mimics. The intergroup differences in Luc/R-Luc values were detected by a dual-luciferase reporter assay system to investigate whether the binding of miR-638 and STARD10 is specific. HepG2 cells were transfected with the miR-638 mimics, miR-638 inhibitor, or control to determine the changes in STARD10 expression at the protein level.

Animal experiment

Mice: All mice passed the 1-week adaptation period under the same conditions. Then began a high-fat diet (containing 21% fat and 0.3% cholesterol). The high-fat diet continued for 28 weeks, and then changed to a normal diet. Subsequently, a completely randomized group design was adopted, and mice were divided into 5 groups of 7 mice each, which were treated as follows: baseline group (n = 7), high-fat diet for 28 weeks; PBS control group (n = 7), High-fat diet was fed for 28 weeks, and then changed to ordinary diet, and PBS was injected into the tail vein; Adenovirus control group (n = 7), high-fat diet was fed for 28 weeks, and then changed to ordinary diet, and adenovirus was injected into the tail vein; StarD10 inhibitors group (n = 7), fed on a high-fat diet for 28 weeks, and then changed to ordinary diet feeding, tail vein injection of lentiviral packaging StarD10 inhibitors vector; StarD10 mimics group (n = 7), high-fat diet fed 28. After that, the mice were switched to the normal diet, and the tail vein was injected with lentiviral packaging StarD10 mimics vector. After 4 weeks, the mice were taken off the eyeballs to measure blood lipids.

Determination of blood lipids: The mice were taken out of the eyeballs to take blood, left to stand, centrifuged (3000 rpm, 20 min), and the supernatant was stored at -80ºC. TG, TC, HDL-C, LDL-C levels and HDL subclasses were detected by Hitachi 7180 automatic analyzer.

Cholesterol reverse transport assay: ^{3}H-cholesterol-labeled macrophages were injected into the abdominal cavity of mice, and the RCT efficiency of the mice was evaluated by measuring the percentage of ^{3}H radioactivity in the total injection activity in serum, liver, and feces. Before macrophages were injected into mice, incubate ^{3}H-cholesterol with acetylated low-density lipoprotein (Ac-LDL) for 30 minutes

to ensure effective binding of ^{3}H-cholesterol and Ac-LDL. It is also necessary to ensure that the proportion of ^{3}H-cholesterol counts in macrophages is greater than 95%. The mice with successful model were injected intraperitoneally with the above suspension, 0.5mL/head, and caged separately for 48h. Blood treatment: Blood was collected from the internal iliac vein 6h, 24h, and 48h after injection of the cell suspension; 12000 r/mim, 10 min; Take 10 μ l plasma and add 5 ml of scintillation solution, and the radioactivity was counted by a liquid scintillation counter; Analysis of total ^{3}H radiation activity in mice blood, and calculate the total blood radioactivity/total radioactivity ratio. Liver treatment: accurately weigh 100 mg frozen liver tissue, homogenize, extract, add n-hexane/isopropanol (3: 2) for extraction, shake for 10 min, collect the supernatant, and vacuum dry; LSC: add scintillation solution 2mL, counting radioactivity with liquid scintillation counter; Total ^{3}H radioactivity of mouse liver was analyzed, and total liver radioactivity/total radioactivity ratio was calculated. Feces disposal: Collect all feces of mice caged for 0-48h, pick them up to EP tubes with tweezers; Dissolve feces: weigh, grind, add 50% ethanol to dissolve feces (1g / 10mL), and mix thoroughly 1-2 min; Take 200 μL of the above fecal mixture, shake it thoroughly with 10 mL of liquid scintillation liquid, and leave it overnight; shake the stool thoroughly again the next day, and liquid scintillation counter to count the radioactivity of feces; and calculate the total fecal radioactivity / total radioactivity ratio.

Western Blot analysis: liver tissue was washed with cold TBS 2-3 times to remove blood stains, cut into small pieces and placed in a homogenizer. Add 10 volumes of tissue volume (add protease inhibitor several minutes before use) and homogenize thoroughly on ice. Transfer the homogenate to a 1.5 ml centrifuge tube , shake, ice bath for 30min. Repeat pipetting with a pipette to ensure complete cell lysis. Centrifuge at 12,000 g for 5 min. Collect the supernatant to obtain the total protein solution. Protein concentration was determined using a modified Bradford method.

Effect of StarD10 on aortic plaque in mice: Collect mouse aortic specimens and observe the effect of StarD10 gene inhibitors vector on the degree and properties of atherosclerosis: Representative aortic sinus sections were selected, and HE staining was used to quantitatively determine the area of atherosclerotic plaques before and after StarD10 expression vector intervention; oil red O staining was used to measure lipid deposition; immunohistochemical staining was used to observe plaque stability indicators: CD68 + giant Phage distribution.

Declarations

Ethics approval and consent to participate: The study was approved by the ethics committee of the People's Liberation Army General Hospital, and each subject provided informed written consent.

Consent for publication: Not applicable.

Competing interests: The authors declare that they have no competing interests.

Funding: This research is supported by the grant from the Key National Basic Research Program of China (2012CB517503, 2013CB530804) and the Key Science and Technology Foundation of China

(2012ZX09303004-002) to Dr. Ping Ye. This research is supported by the Key Science and Technology Foundation of China (2020YFC2004805) to Dr. Sheng Li.

Authors' contributions: XW, PY and YB designed the study; XW, JH and RC

carried out experiments; XW and PY researched and evaluated the literature; XW undertook the statistical analysis and wrote the first draft of the manuscript. All authors read and approved the final manuscript

Acknowledgements: Acknowledgments and disclosures: We thank colleagues at the Department of Laboratory Medicine, the PLA General Hospital for help with biochemical measurements. We are also grateful to all study participants for their participation in the study.

References

1. Castelli WP, Doyle JT, Gordon T, et al. HDL cholesterol and other lipids in coronary heart disease. The cooperative lipoprotein phenotyping study. circulation. 1977; 55:767-72.
2. Mora S, Buring JE, Ridker PM, et al. Association of high-density lipoprotein cholesterol with incident cardiovascular events in women, by low-density lipoprotein cholesterol and apolipoproteinB100 levels: a cohort study. Ann Intern Med. 2011; 155:742-50.
3. Bai Y, Ye P, Luo L, et al. Arterial stiffness is associated with minimally elevated high-sensitivity cardiac troponin T levels in a community-dwelling population. Atherosclerosis. 2011; 218:493-8.
4. Miao DM, Ye P, Xiao WK, et al. Influence of low high-density lipoprotein cholesterol on arterial stiffening and left ventricular diastolic dysfunction in essential hypertension. J Clin Hypertens (Greenwith). 2011;13:710-5.
5. Wang X, Li S, Bai Y, et al. Inverse association of plasma level of high-density lipoprotein cholesterol with intracerebral hemorrhage. J Lipid Res. 2011;52:1747-54.
6. Najafi-Shoushtari SH, Kristo F, Li Y, et al. MicroRNA-33 and the SREBPhost genes cooperate to control cholesterolhomeostasis.2010; 18; 328 (59 85):1566-9.
7. Zampetaki A, Kiechl S, Drozdov I, et al. Plasma microRNA profiling reveals loss of endothelial miR-126 and other microRNAs in type 2 diabetes. Circ Res. 2010; 107(6):810-817.
8. Gupta SK, Bang C, Thum T. Circulating microRNAs as biomarkers and potential paracrine mediators of cardiovascular disease. Circ Cardiovasc Genet. 2010;3(5):484-488.
9. Rodriguez A, Griffiths JS, Ashurst JL, et al. Identification of mammalian miRNA host genes and transcription units. Genome Res. 2004;14(10A): 1902-1910.
10. Ambros V. The functions of animal microRNAs. Nature. 2004; 431 (700 6): 350-355.
11. Aryal B, Singh AK, Rotllan N, et al. MicroRNAs and lipid metabolism. Curr Opin Lipidol. 2017 Jun;28(3):273-280.
12. Wang LP, Gao YZ, Song B, et al MicroRNAs in the Progress of Diabetic Nephropathy: A Systematic Review and Meta-Analysis. Evid Based Complement Alternat Med. 2019 Mar 7; 2019:3513179.

13. Ouimet M, Ediriweera H, Afonso MS, et al. microRNA-33 Regulates Macrophage Autophagy in Atherosclerosis. Arterioscler Thromb Vasc Biol. 2017;37(6):1058-1067.
14. Najafi-Shoushtari SH, Kristo F, Li Y,et al. MicroRNA-33 and the SREBP hostgenes cooperate to control cholesterolhomeostasis. 2010; 18; 328 (5985):1566-9.
15. Rayner KJ, Sheedy FJ, Esau CC, et al. Antagonism of miR-33 in mice promotes reverse cholesterol transport andregression of athe rosclerosis. J Clin Invest.2011; 121(7):2921-31.
16. Rayner KJ, Suárez Y, Dávalos A, Parathath S, MiR-33 contributes to theregulation of cholesterol homeostasis. 2010;18; 328 (59 85):1570-3.
17. Gerin I, Clerbaux LA, Haumont O, et al. Expression of miR-33 from an SREBP2 intron inhibits cholesterol export and fatty acid oxidation. J Biol Chem. 2010; 285(44):33652-33661.
18. Davalos A, Goedeke L, Smibert P, et al. miR -33a/b contribute to the regulation of fatty acid metabolism and insulin signaling. Proc Natl Acad Sci USA. 2011; 108(22):9232-9237.
19. Rayner KJ, Esau CC, Hussain FN, et al. Inhibition of miR-33a/b in non-human primates raises plasma HDL and lowers VLDL triglycerides. 2011; 19;478(7369):404-7.
20. Baselga-Escudero L, Blade C, Ribas-Latre A, et al. Chronic supplementation of proanthocyanidins reduces postprandial lipemia and liver miR-33a and miR-122 levels in a dose-dependent manner in healthy rats. J Nutr Biochem. 2014;25(2):151-156.
21. Moore KJ, Rayner KJ, Suárez Y, et al. The role of microRNAs in cholesterol efflux and hepatic lipid metabolism. Annu Rev Nutr. 2011; 31:49-63.
22. Tsai WC, Hsu SD , Hsu CS , et al. MicroRNA-122 plays a critical role in liver homeostasis and hepatocarcinogenesis. J Clin Invest. 2012, 122 (8): 2884-2897.
23. Hsu SH, Wang B , Kota J , et al. Essential metabolic, antiinflamma-tory , and anti-tumorigenic functions of miR-122 in liver. J Clin Invest. 2012; 122 (8): 2871-2883.
24. Iliopoulos D, Drosatos K, Hiyama Y, et al. MicroRNA-370 controls the expression of MicroRNA-122 and Cpt1 alpha and affects lipid metabolism. J Lipid Res. 2010;51(6):1513-1523.
25. Moore KJ, Rayner KJ, Suárez Y, et al. The role of microRNAs in cholesterol efflux and hepatic lipid metabolism. Annu Rev Nutr. 2011; 31:49-63.
26. Zhang M, Wu JF, Chen WJ, et al. MicroRNA-27a/b regulates cellular cholesterol efflux, influx and esterification/hydrolysis in THP-1 macrophages. Atherosclerosis. 2014; 234(1):54-64.
27. Nakanishi N, Nakagawa Y, Tokushige N, et al. The up-regulation of microRNA-335 is associated with lipid metabolism in liver and white adipose tissue of genetically obese mice[J].Biochemical and Biophysical Research Communications. 2009; 385:492-496.
28. Esau C, Kang X, Peralta E, et al. MicroRNA-143 regulates adipocyte differentiation [J].Journal of Biological Chemistry. 2004; 279 (50): 52 361-52365.
29. Wang X, Lu Y, Zhu L, et al. Inhibition of miR-27b Regulates Lipid Metabolism in Skeletal Muscle of Obese Rats During Hypoxic Exercise by Increasing PPARγ Expression. Front Physiol. 2020 Aug

31;11:1090.

30. Luque A, Farwati A, Krupinski J, et al. Association between low levels of serum miR-638 and atherosclerotic plaque vulnerability in patients with high-grade carotid stenosis. J Neurosurg. 2018 Jul 27;131(1):72-79.
31. Lin QY, Wang JQ, Wu LL, et al. miR-638 represses the stem cell characteristics of breast cancer cells by targeting E2F2. Breast Cancer. 2020 Jan;27(1):147-158.
32. Duong PT, Collins HL, Nickel M, et al. Characterization of nascent HDL particles and microparticles formed by ABCA1-mediated efflux of cellular lipids to apoA-I. J Lipid Res 2006; 47:832–843.
33. Karlsson H, Leanderson P, Tagesson C, et al. Lipoproteomics II: mapping of proteins in high-density lipoprotein using two-dimensional gel electrophoresis and mass spectrometry. Proteomics 2005; 5:1431–1445.
34. Gordon DJ, Probstfield JL, Garrison RJ, et al. High-density lipoprotein cholesterol and cardiovascular disease. Four prospective American studies [J]. Circulation, 1989, 79:8-15.
35. Vedhachalam C, Duong PT, Nickel M, et al. Mechanism of ATP-binding cassette transporter A1-mediated cellular lipid efflux to apolipoprotein A-I and formation of high density lipoprotein particles. J Biol Chem 2007; 282:25123–25130.
36. Gelissen IC, Harris M, Rye KA, et al. ABCA1 and ABCG1 synergize to mediate cholesterol export to apoA-I. Arterioscler Thromb Vasc Biol 2006; 26:534–540.
37. Tarling EJ, Edwards PA. ATP binding cassette transporter G1 (ABCG1) is an intracellular sterol transporter. Proc Natl Acad Sci USA 2011; 108:19719–19724.
38. Baldan A, Tarr P, Vales CS, et al. Deletion of the transmembrane transporter ABCG1 results in progressive pulmonary lipidosis. J Biol Chem 2006; 281:29401–29410.
39. Westerterp M, Murphy AJ,Wang M, et al. Deficiency of ATP-binding cassette transporters A1 and G1 in macrophages increases inflammation and accelerates atherosclerosis in mice. Circ Res 2013; 112:1456–1465.
40. Barter PJ, Caulfield M, Eriksson M, et al. ILLUMINATE Investigators: Effects of torcetrapib in patients at high risk for coronary events. N Engl J Med. 2007; 22: 357 (21):2109-22.
41. Tardif JC, Rhéaume E, Lemieux Perreault LP, et al. Pharmacogenomic determinants of the cardiovascular effects of dalcetrapib. Circ Cardiovasc Genet. 2015; 8(2):372-82.
42. The HPS2-THRIVE Collaborative Group. Effects of Extended-Release Niacin with Laropiprant in High-Risk Patients. N Engl J Med. 2014; 371:203-212.
43. Movva R, Rader DJ. Laboratory assessment of HDL heterogeneity and function. Clin Chem. 2008; 54(5):788-800.
44. Fuhrman B, Gantman A, Aviram M, et al. Paraoxonase 1(PON1) deficiency in mice is associated with reduced expression of macrophage SR-BI and consequently the loss of HDL cytoprotection against apoptosis. Atherosclerosis. 2010; 211:61-68.

45. Tian L,Fu M.The relationship between high density lipoprotein subclass profile and plasmalipids concentration. Lipids Health Dis. 2010; 9:118-118.
46. Julia Z, Duchene E, Fournier N, et al. Postprandial lipemia enhances the capacity of large HDL2 particles to mediate free cholesterol efflux via SR-BI and ABCG1 pathways in type IIB hyperlipidemia. J Lipid Res. 2010; 51:3350-3358.
47. Shuhei N, Söderlund S, Jauhiainen M, et al. Effect of HDL composition and particle size on the resistance of HDL to the oxidation. Lipids Health Dis. 2010; 9:104-104.
48. Rosenson RS, Brewer HB Jr, Chapman MJ, et al. HDL measures, particle heterogeneity, proposed nomenclature, and relation to atherosclerotic cardiovascular events. Clin Chem.2011;57:392-410.
49. L Ulf. Coronary artery disease: HDL and coronary heart disease-novel insights. Nature Reviews Cardiology. 2014; 11(10):559-560.
50. Fernandez-Hernando C, Ramirez CM, Goedeke L, et al. MicroRNAs in metabolic disease. Arterioscler Thromb Vasc Biol 2013; 33:178-185.
51. Fernandez-Hernando C, Suarez Y, Rayner KJ, et al. MicroRNAs in lipid metabolism. Curr Opin Lipidol 2011; 22:86-92.
52. Moore KJ, Rayner KJ, Suarez Y, et al. microRNAs and cholesterol metabolism. Trends Endocrinol Metab 2010; 21:699-706.
53. Marquart TJ, Allen RM, Ory DS, et al miR-33 links SREBP-2 induction to repression of sterol transporters. Proc Natl Acad Sci USA 2010; 107:12228-12232.
54. Najafi-Shoushtari SH, Kristo F, Li Y, et al. MicroRNA-33 and the SREBP host genes cooperate to control cholesterol homeostasis. Science 2010; 328:1566-1569.
55. Rayner KJ, Suarez Y, Davalos A, et al. MiR-33 contributes to the regulation of cholesterol homeostasis. Science 2010; 328:1570-1573.
56. Davalos A, Goedeke L, Smibert P, et al. miR-33a/b contribute to the regulation of fatty acid metabolism and insulin signaling. Proc Natl Acad Sci USA 2011; 108:9232-9237.
57. Allen RM, Marquart TJ, Albert CJ, et al. miR-33 controls the expression of biliary transporters, and mediates statin and diet-induced hepatotoxicity. EMBO Mol Med 2012; 4:882-895.
58. Horie T, OnoK, Horiguchi M, et al. MicroRNA-33 encoded by an intron of sterol regulatory element-binding protein 2 (Srebp2) regulates HDL in vivo. Proc Natl Acad Sci USA 2010; 107:17321-17326.
59. Rayner KJ, Esau CC, Hussain FN, et al. Inhibition of miR-33a/b in nonhuman primates raises plasma HDL and lowers VLDL triglycerides. Nature 2011; 478:404-407.
60. Rottiers V, Obad S, Petri A, et al. Pharmacological inhibition of a microRNA family in nonhuman primates by a seed targeting 8-mer antimiR. Sci Transl Med 2013; 5:212.

Tables

Table 1 Body weight and liver weight of mice in different groups（n=7， $\bar{x}$ ±s）

	weight（g）	Liver（g）
Baseline group	24.51±0.81	1.49±0.14
PBS group	24.37±1.88	1.43±0.12
Adenovirus control group	25.12±1.15	1.49±0.10
StarD10 inhibitors group	23.99±1.01	1.53±0.15
StarD10 mimics group	24.62±1.12	1.57±0.13

Table 2 Effect of StarD10 on HDL subtypes in mice ($\bar{x}$ ±s,mmol/L,n=7)

	Baseline group	PBS group	Adenovirus control group	StarD10 inhibitors group	StarD10 mimics group
HDL2-C	0.72±0.31	1.62±0.26	1.23±0.15	1.06±0.24	0.69±0.28*
HDL3-C	0.33±0.03	0.42±0.09	0.57±0.19	0.63±0.10	0.46±0.17*
HDL2-C/HDL-C(%)	65.9±8.91	79.2±4.42	68.6±7.21	59.3±9.50	59.8±5.59
HDL3-C/HDL-C(%)	34.1±8.32	20.7±3.91	30.9±7.14	40.7±4.67*	38.2±5.86*

*P<0.05, the HDL3-C / HDL-C ratio was increased in the StarD10 inhibitors group compared with the baseline group, the PBS control group, and the adenovirus control group, and there was a statistical difference. The HDL2-C and HDL3-C concentrations in the StarD10 mimics group decreased, the HDL3-C / HDL-C ratio increased, there are statistical differences

Table 3 Changes of ^{3}H-cholesterol distribution in serum of mice in each group (n=7，cpm%)

^{3}H content	PBS control group	Adenovirus control group		StarD10 inhibitors group	StarD10 mimics group
6h plasma	1.105	1.324	1.343		1.1737
24h plasma	2.929	3.052	3.555		2.8562
48h plasma	6.142	6.090	9.816**		6.2587
**P<0.01					

Table4 Distribution of residual ^{3}H-cholesterol in liver and feces of mice in each group (n = 7, cpm%)

	liver（cpm%）	feces（cpm%）
PBS control group	3.151	1.988
Adenovirus control group	3.309	1.874
StarD10 inhibitors group	4.326**	1.862**
StarD10 mimics group	3.501	1.917
**P<0.01		

Figures

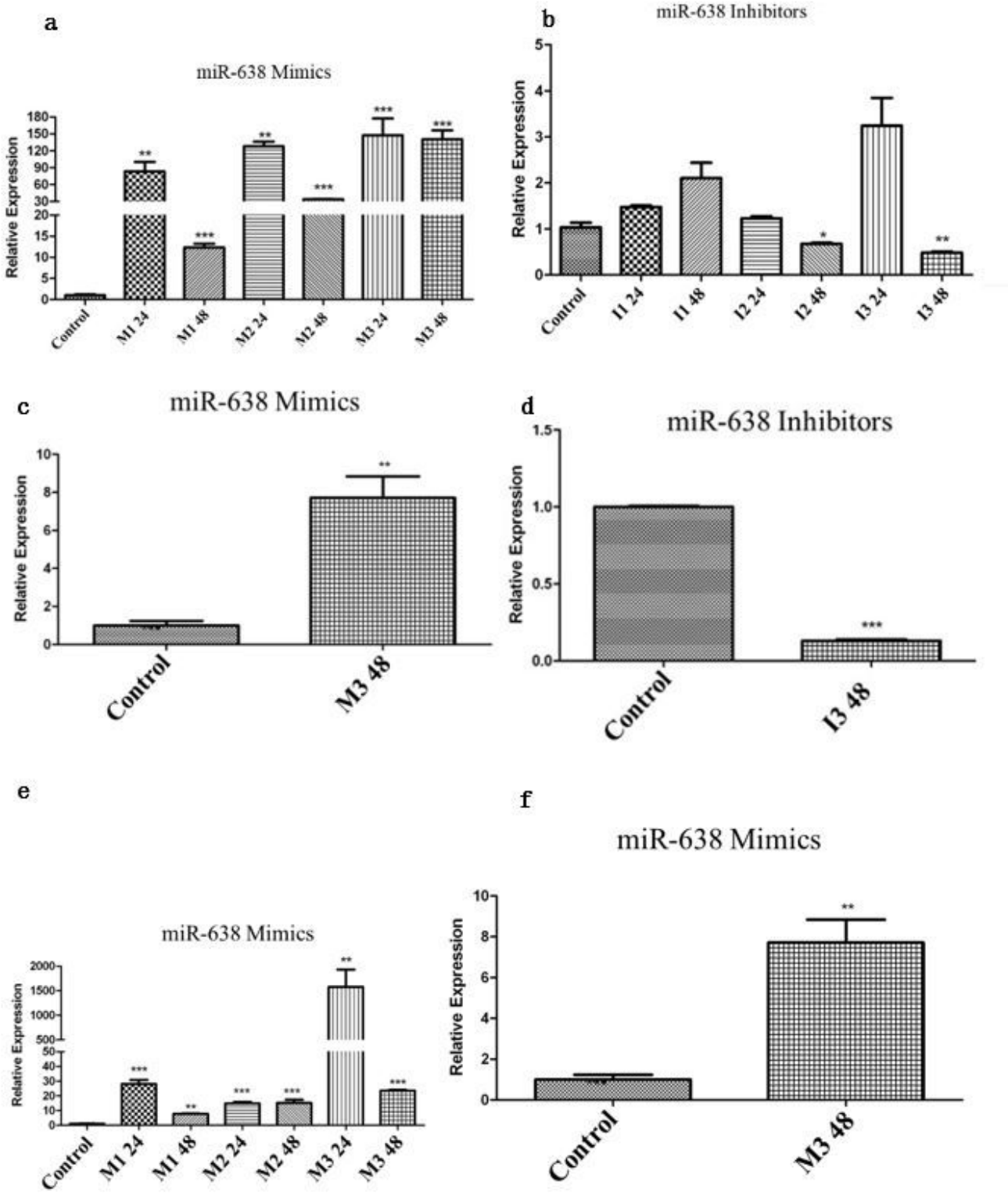

Figure 1

Relative expression of mir-638 in HepG2/ macrophages cells treated with mir-638 Mimics / inhibitors (n=3). a: Relative expression of miR-638 in each group after treatment of HepG2 cells with different concentrations of miR-638 Mimics (n=3); b: Relative expression of miR-638 in each group after treatment of HepG2 cells with different concentrations of miR-638 inhibitors (n=3); c: mir-638 Mimics in HepG2; d: mir-638 inhibitors in HepG2; e: Relative expression of miR-638 in each group after treatment of

macrophages cells with different concentrations of miR-638 Mimics (n= 3); f:mir-638 Mimics in macrophages

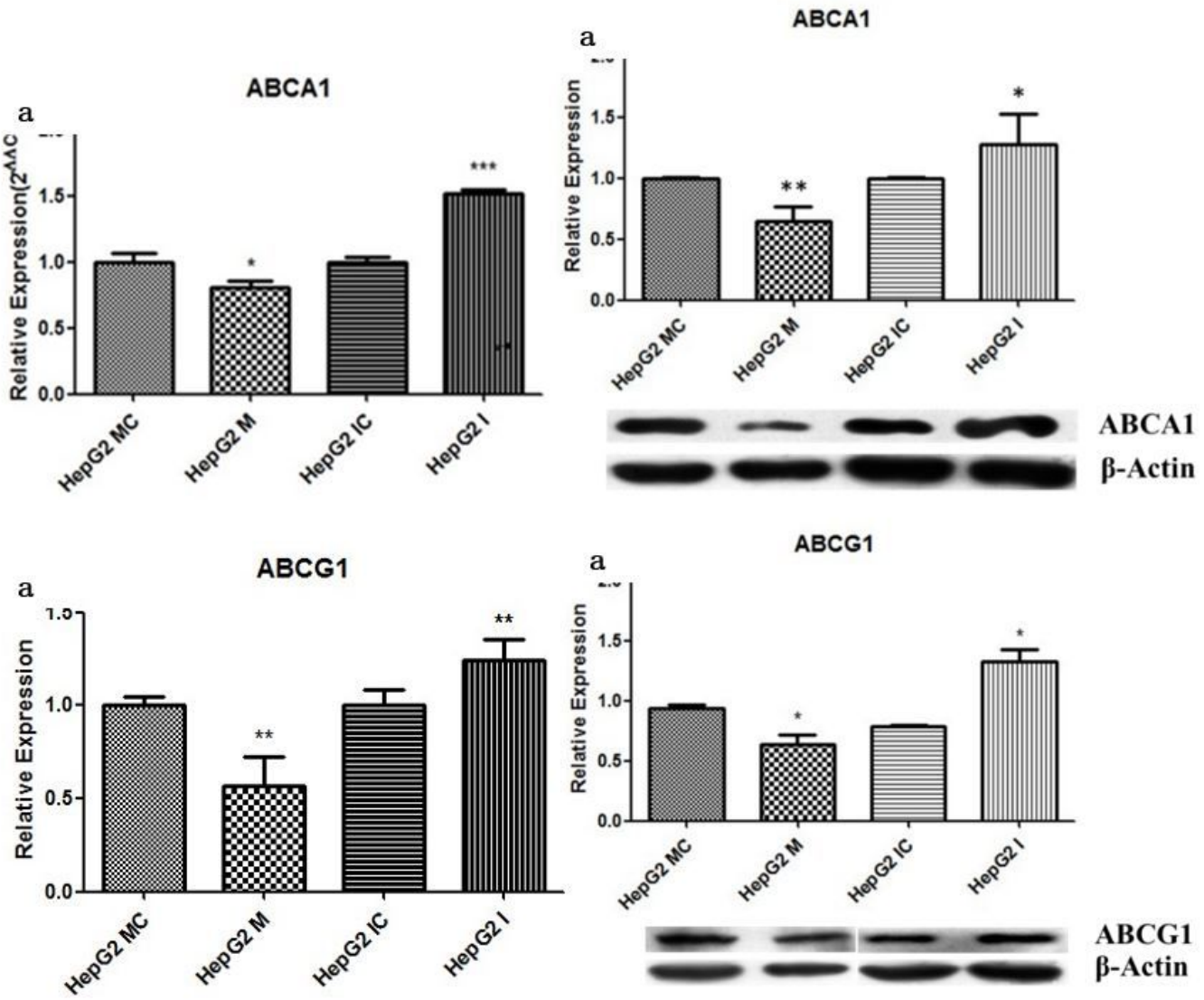

Figure 2

changes of ABCA1 and ABCG1 RNA / protein level after mir-638 mimics / inhibitors transfection into HepG2 cells (n=3). a: ABCA1 RNA level in HepG2 cells; b: ABCA1 protein level in HepG2 cells; c: ABCG1 RNA level in HepG2 cells; d: ABCA1 protein level in HepG2 cells protein

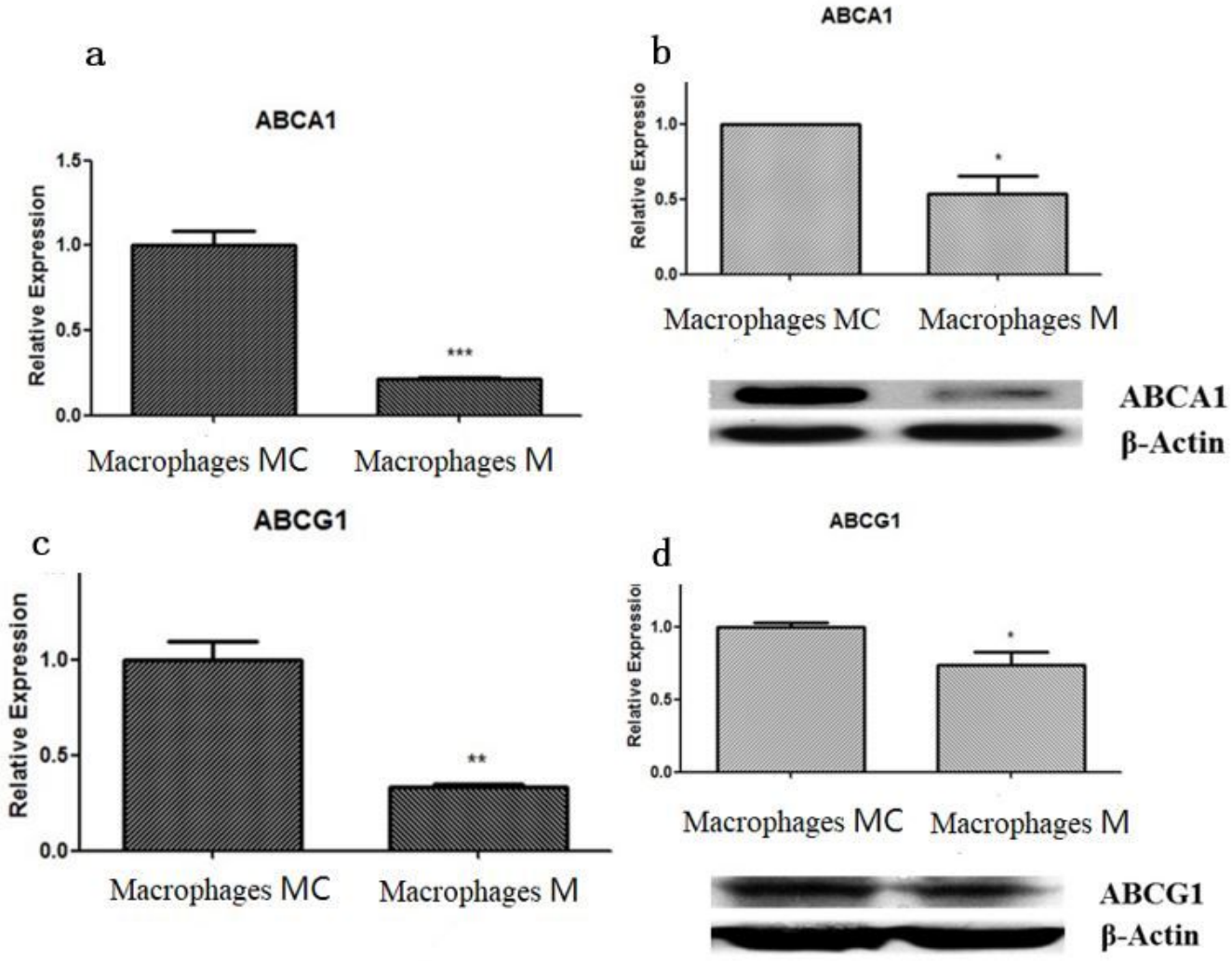

Figure 3

changes of ABCA1 and ABCG1 RNA / protein level after mir-638 mimics / inhibitors transfection into macrophages cells (n=3). a: ABCA1 RNA level in macrophages cells; b: ABCA1 protein level in macrophages cells; c: ABCG1 RNA level in macrophages cells; d: ABCA1 protein level in macrophages cells protein

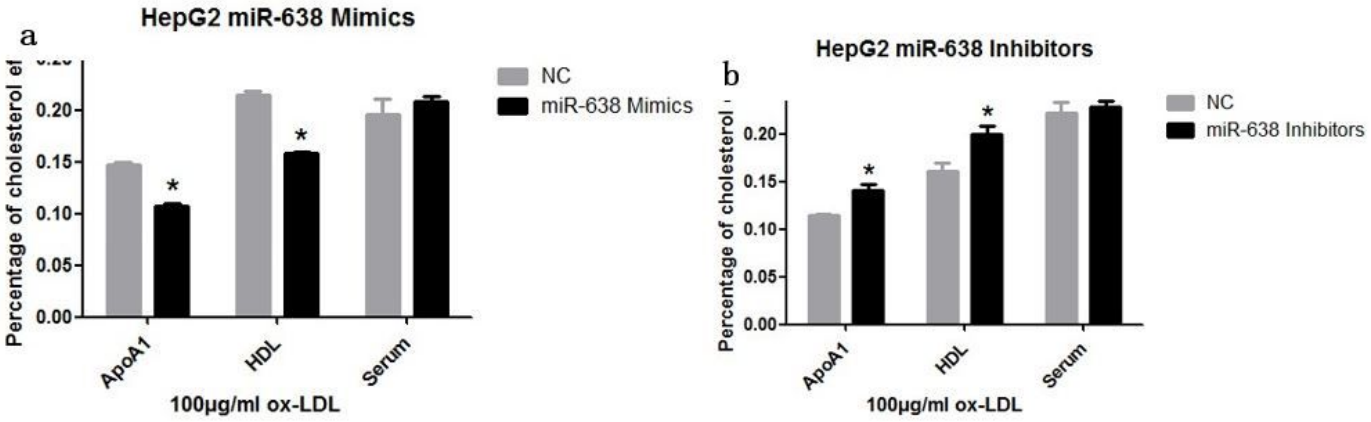

Figure 4

NBD cholesterol outflow rate of HepG2 cells transfected with mir-638 mimics / inhibitors (n = 3)

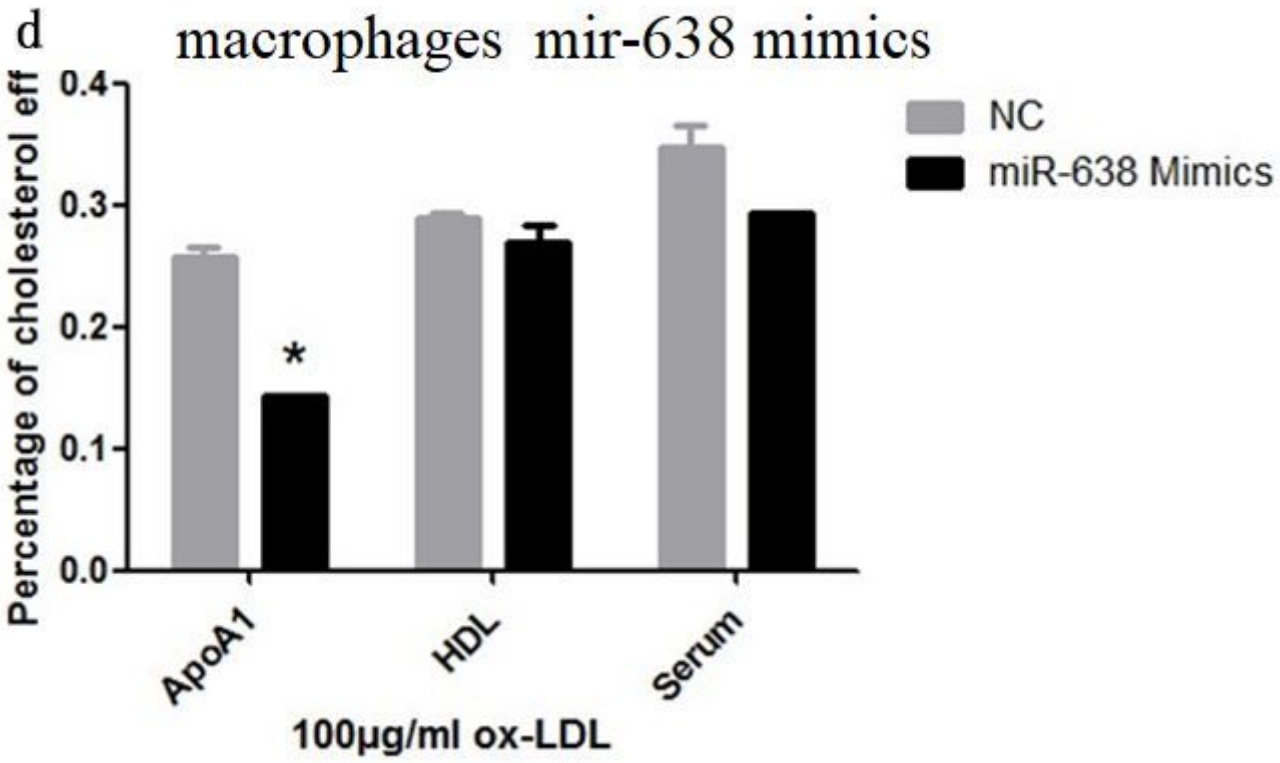

Figure 5

NBD cholesterol outflow rate of macrophages cells transfected with mir-638 mimics (n = 3)

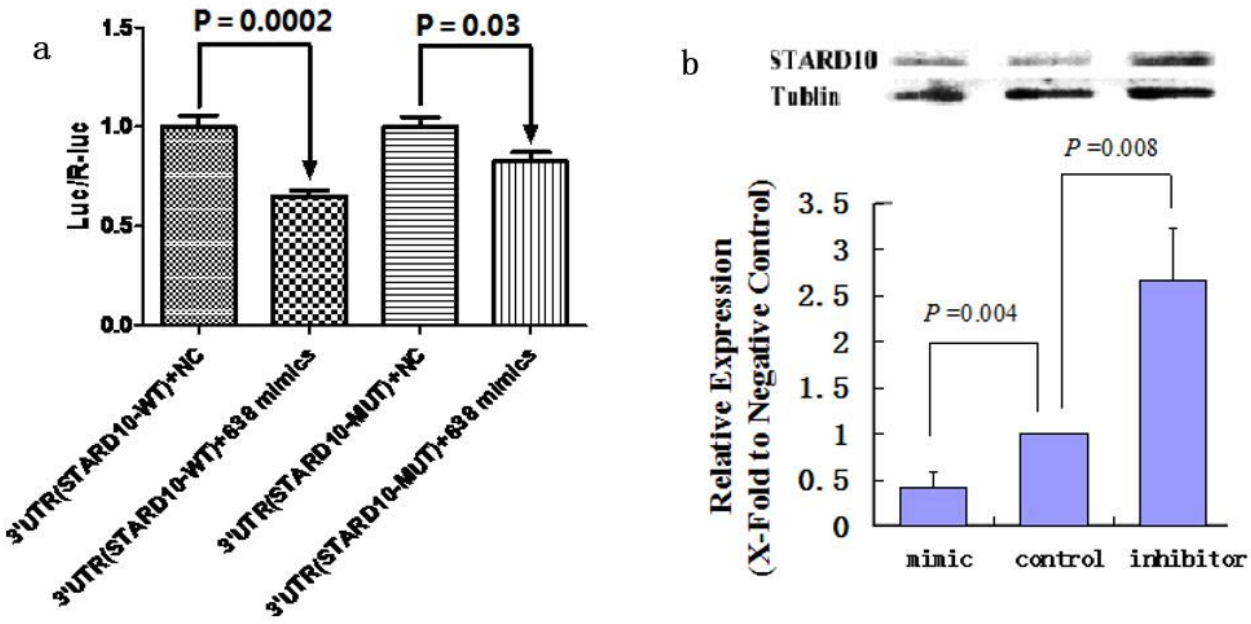

Figure 6

a: miR-638 combined with STARD10 specifically, after mutation of this binding site, the regulatory relationship between mir-638 and StarD10 becomes weaker. b: Over expression of miR-638 downregulated the expression of STARD10 protein, and inhibition of miR-638 upregulated the expression of STARD10 protein.

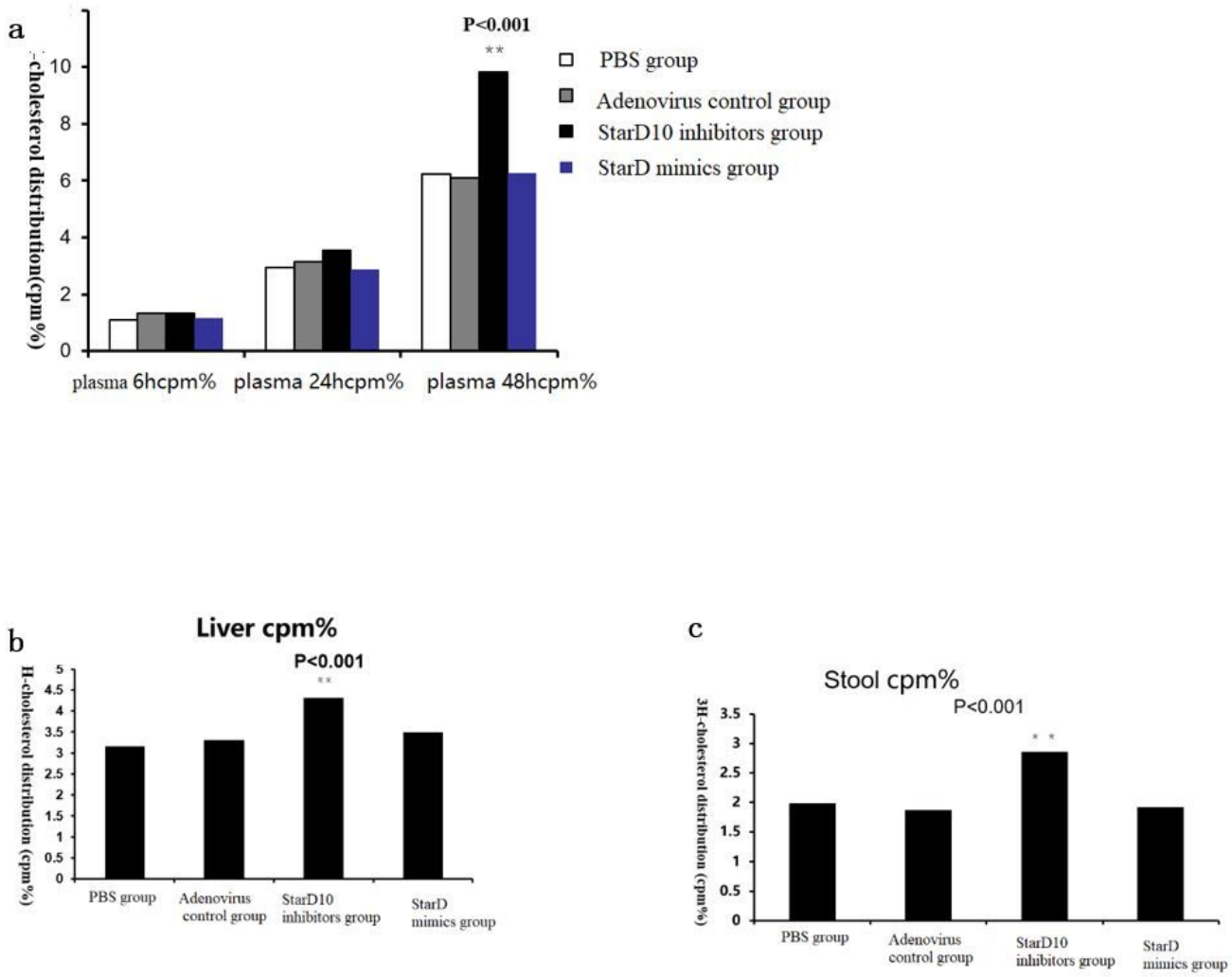

Figure 7

a: Distribution of serum 3H-cholesterol at 6h, 24h and 48h in each group of mice(n = 7, cpm%), ** P <0.01; b: Distribution of liver 3H-cholesterol at 48h in each group of mice (n = 7, cpm%), ** P <0.01; c: 3H-cholesterol distribution in mice at and 48h (n = 7, cpm%), ** P <0.01

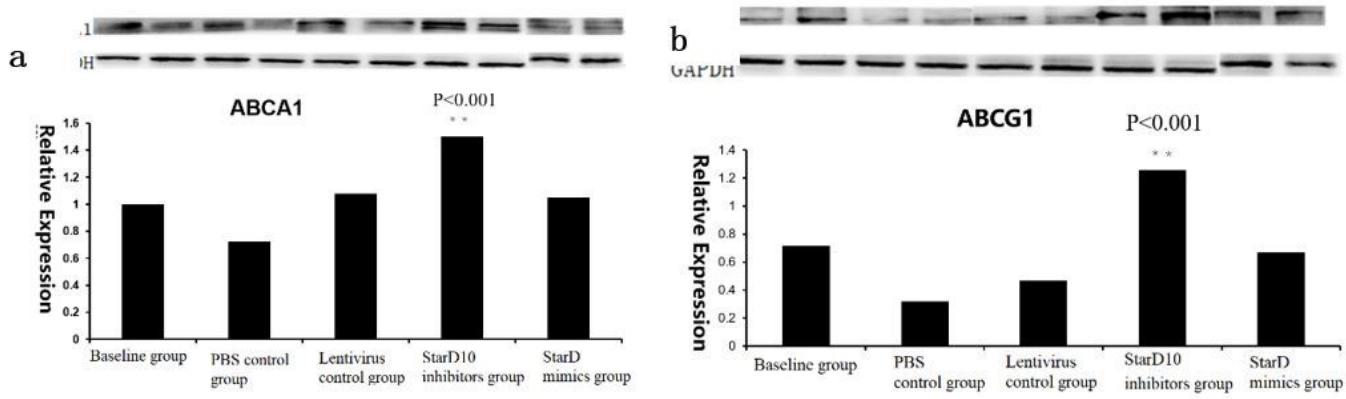

Figure 8

a: ABCA1 protein expression in liver tissue (n=7). The figure above shows the electrophoresis of ABCA1 protein in liver tissue. The figure below is a semi-quantitative analysis of ABCA1 protein expression. ** P <0.01; b: ABCG1 protein expression in liver tissue (n=7). The figure above shows the electrophoresis of ABCG1 protein in liver tissue. The figure below is a semi-quantitative analysis of ABCG1 protein expression. ** P <0.01.

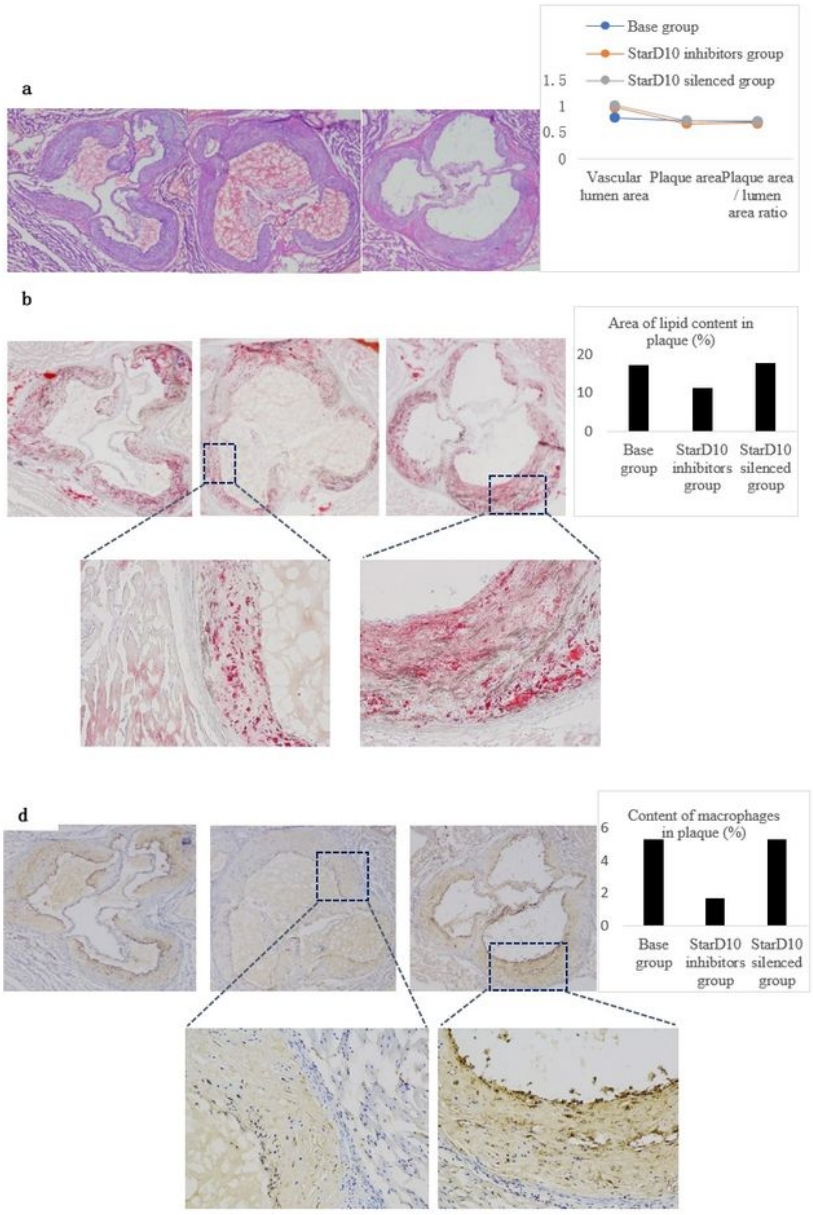

Figure 9

a: Representative hematoxylin- and eosin-stained aortic sinus sections from StarD10 inhibitors group and StarD10 mimics group(Original magnification: ×40); b:Oil red O staining for neutral lipids. Original magnification: ×40 (top images); ×200 (bottom images); c: immunohistochemical staining for the macrophage marker CD68. Original magnification: ×40 (top images); ×200 (bottom images).